

# Searching for double-peak and doubly broken gravitational-wave spectra from Advanced LIGO-Virgo's first three observing runs

Wang-Wei Yu<sup>1,2\*</sup> and Shao-Jiang Wang<sup>1†</sup>

<sup>1</sup>CAS Key Laboratory of Theoretical Physics, Institute of Theoretical Physics,  
Chinese Academy of Sciences, Beijing 100190, China

<sup>2</sup>School of Physical Sciences, University of Chinese Academy of Sciences (UCAS), Beijing 100049, China

The current LIGO-Virgo observing run has been pushing the sensitivity limit to touch the stochastic gravitational-wave backgrounds (SGWBs). However, no significant detection has been reported to date for any single dominated source of SGWBs with a single broken-power-law (BPL) spectrum. Nevertheless, it could equally well escape from existing Bayesian searches from, for example, two comparable dominated sources with two separate BPL spectra (double-peak case) or a single source with its power-law behavior in the spectrum broken twice (doubly broken case). In this paper, we put constraints on these two cases but specifically for the model with cosmological first-order phase transitions from Advanced LIGO-Virgo's first three observing runs. We found strong negative evidence for the double-peak case and hence place 95% C.L. upper limits  $\Omega_{\text{BPL},1} < 5.8 \times 10^{-8}$  and  $\Omega_{\text{BPL},2} < 4.4 \times 10^{-8}$  on the two BPL spectra amplitudes with respect to the unresolved compact binary coalescence (CBC) amplitude  $\Omega_{\text{CBC}} < 5.6 \times 10^{-9}$ . We further found weak negative evidence for the doubly broken case and hence place 95% C.L. upper limit  $\Omega_{\text{DB}} < 1.2 \times 10^{-7}$  on the overall amplitude of the doubly broken spectrum with respect to  $\Omega_{\text{CBC}} < 6.0 \times 10^{-9}$ . In particular, the results from the double-peak case have marginally ruled out the strong super-cooling first-order phase transitions at LIGO-Virgo band.

## I. INTRODUCTION

The sensitivity limits have been persistently pushed forward during the first three observing runs (O1 [1], O2 [2], and O3 [3]) of the Advanced LIGO [4] and Advanced Virgo [5] gravitational wave (GW) detectors, which might uncover the stochastic GW backgrounds (SGWBs) [6–8] from unresolved sources of both astrophysical and cosmological origins. The unresolved sources of astrophysical origins mainly consist of the compact binary coalescences (CBCs) from unresolved individual sources such as binary black hole and neutron star mergers [9–13] as well as other more exotic sources that are also more difficult to be observed, including the core-collapse supernovae [14–17], rotating neutron stars [18–24], stellar-core collapses [25–27], and boson clouds around black holes [28–34], to name just a few.

The SGWBs of cosmological origins [35] can embrace much more rich physics [36, 37]. Primordial GWs produced from an inflationary era [38] uniquely mark the energy scale of cosmic inflation, in particular, the scalar-induced secondary GWs [39–43] during inflation depict the curvature perturbations at small scales. The SGWBs from cosmological first-order phase transitions (FOPTs) [44–48] and cosmic strings [49–52] necessarily encode the new physics beyond the standard model of particle physics, while the SGWBs from primordial black hole (PBH) mergers [53] can constrain the PBH abundance in the dark matter. However, multiple sources of these SGWBs of cosmological origins can be equally well present simultaneously in the GW data.

The detectability for SGWBs below the confusion limit is by no doubt difficult compared to the individually resolvable GW events that make up a tiny fraction of all GW signals present in the detector time stream. The most recent isotropic search [54] from O3 combined with previous ones from O1 [55] and O2 [56] is consistent with uncorrelated noise and hence places upper limits on the normalized GW energy density for power-law spectral-index values of 0 (flat), 2/3 (CBCs), and 3 (causality). Other efforts of searches with LIGO-Virgo Collaboration for the SGWBs from cosmic strings [57, 58], FOPTs [59–62], and induced GWs [63, 64] all return a null result.

However, a simple Bayesian search with a single broken power-law (BPL) spectrum for any single but dominated source of SGWBs might just miss possible detections on, for example, two comparable dominated sources of SGWBs with two separate single-BPL spectra (double-peak case) or a single source of SGWBs with its power-law behavior in the spectrum broken twice (double-broken case). The double-peak (DP) case also includes a single source of SGWBs but already with two peaks by nature, for example, two-step FOPT [65, 66], one-step FOPT but with comparable GWs from both wall collisions and sound waves when bubbles collide during the transition to a near constant terminal wall velocity [67], induced GWs with two peaks for some particular configuration on curvature perturbations [68], oscillons with cuspy potentials [69] during preheating era. The doubly broken (DB) case can be found in an analytic evaluation on the GWs from wall collisions beyond the envelope approximation [70] and a hybrid simulation for the sound waves [71] (see also [72]).

In this paper, we search for the SGWB signals in the cases with DP and DB spectra from Advanced LIGO-Virgo's first three observing runs but with a special focus

\* yuwangwei@mail.itp.ac.cn

† Corresponding author: schwang@itp.ac.cn

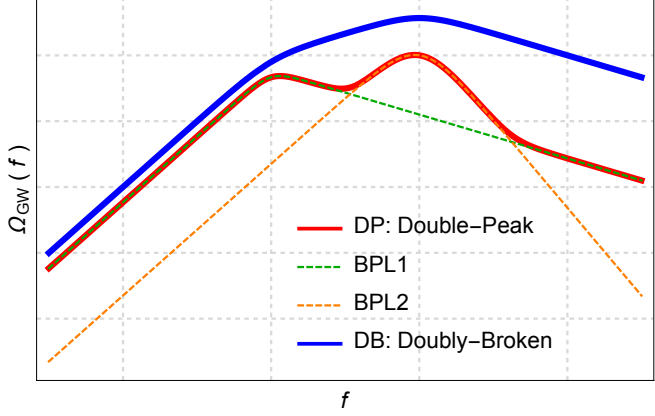


FIG. 1. The schematic comparison between DP (red solid) and DB (blue solid) spectra for the SGWB. The DP spectrum consists of two separate BPL spectra (green and orange dashed) while the DB spectrum admits a three-section power-law scaling.

on SGWBs from FOPTs. The models are introduced in Sec. II and constrained in Sec. III, and the results are summarized in Sec. IV.

## II. MODELS

The BPL spectrum of SGWBs can be modeled as

$$\Omega_{\text{BPL}}(f; \boldsymbol{\theta}) = \Omega_* \left( \frac{f}{f_*} \right)^{n_1} \left[ \frac{1 + (f/f_*)^\Delta}{2} \right]^{(n_2 - n_1)/\Delta} \quad (1)$$

with  $\boldsymbol{\theta} \equiv (\Omega_*, f_*, n_1, n_2, \Delta)$ , where  $\Omega_*$  is the peak amplitude at the peak frequency  $f_*$ ,  $n_1 (= 3$  for causality) and  $n_2$  are the asymptotic slopes on the far left and far right ends of the peak frequency, respectively, and  $1/\Delta$  is the peak transition width. We define the DP spectrum as simply the sum of two separate BPL spectra,

$$\Omega_{\text{DP}}(f; \{\boldsymbol{\theta}_1, \boldsymbol{\theta}_2\}) = \Omega_{\text{BPL}}(f; \boldsymbol{\theta}_1) + \Omega_{\text{BPL}}(f; \boldsymbol{\theta}_2) \quad (2)$$

with  $\boldsymbol{\theta}_i \equiv (\Omega_{*,i}, f_{*,i}, n_{1,i}, n_{2,i}, \Delta_i)$  for the peaks  $i = 1, 2$ , while the DB spectrum is modeled as a three-section power-law scaling by

$$\Omega_{\text{DB}}(f; \boldsymbol{\theta}) = \frac{\Omega_*}{\left(\frac{f}{f_l}\right)^{-n_l} + \left(\frac{f}{f_l}\right)^{-n_m} + \left(\frac{f_h}{f_l}\right)^{-n_m} \left(\frac{f}{f_h}\right)^{-n_h}} \propto \begin{cases} (f/f_l)^{n_l}, & f \ll f_l, \\ (f/f_l)^{n_m}, & f_l \ll f \ll f_h, \\ (f_h/f_l)^{n_m} (f/f_h)^{n_h}, & f_h \ll f, \end{cases} \quad (3)$$

with  $\boldsymbol{\theta} \equiv (\Omega_*, f_l, f_h, n_l, n_m, n_h)$ , where we will assume  $n_l > n_m > n_h$  and  $f_l < f_h$  with a specific example [71] in mind. An explicit comparison between DP and DB spectra is shown in Fig. 1. The reference SGWBs from unresolved CBCs can be approximated by a  $f^{2/3}$  power-

law spectrum [73] in the inspiral phase as

$$\Omega_{\text{CBC}}(f; \boldsymbol{\theta}) = \Omega_{\text{ref}} \left( \frac{f}{f_{\text{ref}}} \right)^{2/3} \quad (4)$$

with  $\boldsymbol{\theta} \equiv (\Omega_{\text{ref}}, f_{\text{ref}})$ , where  $\Omega_{\text{ref}}$  is the reference amplitude at the reference frequency  $f_{\text{ref}}$  that will be fixed at 25 Hz around the most sensitive frequency band of the LIGO-Virgo network. For all the above models, the uncorrelated Gaussian noise is implicitly included with  $\Omega_N(f) = 0$ .

The primary motivation to test above models beyond the simple BPL model comes from SGWBs from FOPTs, which usually occur for breaking some continuous symmetry that would form a potential barrier for the false vacuum decaying into the true vacuum. The vacuum decay process proceeds via spontaneous nucleations of true vacuum bubbles in the false vacuum plasma, followed by rapid expansions of bubble walls until violent collisions, along with which the expanding bubble walls also stimulate fluid motions of the thermal plasma. Therefore, both the bubble wall collisions and plasma fluid motions would generate SGWBs. The simple BPL spectrum with  $n_1 = 3$ ,  $n_2 = -1$ , and  $\Delta = 4$  can depict the GW spectrum from bubble-wall collisions under the dubbed envelope approximation [74], in which case the overlapping parts of thin walls are neglected upon collisions. However, by going beyond the envelope approximation, the analytic modeling [70] of wall collisions reveals a three-section power-law scaling with  $n_l = 3$ ,  $n_m = 1$ , and  $n_h = -1$  that can be described by a DB spectrum. Furthermore, the GWs from plasma fluid motions especially the dominated contributions from sound waves can also be fitted by the simple BPL spectrum with  $n_1 = 3$ ,  $n_2 = -4$ , and  $\Delta = 2$  as suggested by numerical simulations [75–77]. However, analytic modelings [78–80] seem to prefer a DB spectrum with  $n_l = 3$ ,  $n_m = 1$ , and  $n_h = -3$  but still with some uncertainty in determining its high-frequency slope within  $-3 \leq n_h \leq -1$  [80]. Nevertheless, we will stick to the fitting spectrum from numerical simulation instead of the analytic estimation for the sound waves. On the other hand, it is probable for some specific particle physics model of FOPT in its particular parameter space that the contributions from the envelope collisions and sound waves are comparable, which can be described by a DP spectrum.

## III. DATA ANALYSIS

We closely follow the method outlined in Refs. [54, 59, 63] to search for SGWBs in the current GW data. The log-likelihood for the model parameter set  $\boldsymbol{\theta}$  is estimated

TABLE I. The prior choices for the combined SGWB models BPL+CBC, DP+CBC, and DB+CBC.

BPL + CBC		
Parameter	Prior	
$\Omega_{\text{ref}}$	LogUniform ( $10^{-10}, 10^{-7}$ )	
$\Omega_*$	LogUniform ( $10^{-9}, 10^{-4}$ )	
$f_*$	Uniform (0, 256) Hz	
$n_1$	3	
sound waves	envelope-wall collisions	
$n_2$	-4	-1
$\Delta$	2	4
DP + CBC		
Parameter	Prior	
$\Omega_{\text{ref}}$	LogUniform ( $10^{-10}, 10^{-7}$ )	
$\Omega_{*,i}$	LogUniform ( $10^{-9}, 10^{-4}$ )	
$f_{*,1}$	Uniform (0, 256) Hz	
$f_{*,2}(> f_{*,1})$	Uniform (0, 256) Hz	
$n_{1,i}$	3	
$n_{2,1}$	-1	envelope-wall collisions
$n_{2,2}$	-4	sound waves
$\Delta_1$	4	envelope-wall collisions
$\Delta_2$	2	sound waves
DB + CBC		
Parameter	Prior	
$\Omega_{\text{ref}}$	LogUniform ( $10^{-10}, 10^{-7}$ )	
$\Omega_*$	LogUniform ( $10^{-9}, 10^{-4}$ )	
$f_l$	Uniform (0, 256) Hz	
$f_h(> f_l)$	Uniform (0, 256) Hz	
$n_l(> n_m)$	3	beyond envelope wall collisions
$n_m(> n_h)$	1	
$n_h$	-1	

by [81–84]

$$\log p(\hat{C}_{IJ}|\boldsymbol{\theta}, \lambda) \propto -\frac{1}{2} \sum_k \frac{[\hat{C}_{IJ}(f_k) - \lambda \Omega_{\text{GW}}(f_k; \boldsymbol{\theta})]^2}{\sigma_{IJ}^2(f_k)} \quad (5)$$

with the sum  $k$  running over the frequency bins, where  $\hat{C}_{IJ}(f)$  is the cross-correlation statistic for the baseline  $IJ$  with  $I, J = H, L, V$  for the LIGO-Hanford, LIGO-Livingston, and Virgo (HLV) detectors,  $\sigma_{IJ}^2(f)$  is the variance of  $\hat{C}_{IJ}(f)$  in the small signal-to-noise ratio limit [85], and  $\lambda$  accounts for the calibration uncertainties of the detectors [86] that would be eventually marginalized over [87]. Since the current data still favors a pure Gaussian noise model [54], the contribution from Schumann resonances is negligible [83, 88, 89]. The final likelihood is obtained by summing over multiple log-likelihoods for different baselines in order to con-

strain the model parameters. As the SGWB from CBCs is an indispensable part of any SGWBs at the LIGO-Virgo band, we will search for SGWBs specifically from FOPTs for the combined models BPL+CBC, DP+CBC, and DB+CBC with their parameter priors depicted in Table I. For model comparison, we adopt the ratios of evidence  $\log \mathcal{B}_{\text{Noise}}^{i+\text{CBC}}$  and  $\log \mathcal{B}_{\text{CBC}}^{i+\text{CBC}}$  from the Bayes factor to evaluate the preference for a specific SGWB model over a pure Gaussian noise model and a CBC background, respectively.

## IV. RESULTS

The Bayes-ratio comparison of models constrained by the dynamic nested sampling package `dynesty` [90] in BILBY [91] is summarized in Fig. 2, which will be described in details shortly below. The general conclusion is that, the SGWB from a DP spectrum is even more disfavored than the SGWB with a single BPL spectrum or a DB spectrum, but all of which are not detected compared to the backgrounds from either uncorrelated Gaussian noises or CBCs.

### A. The BPL+CBC model

To compare with previous results in the literature, we repeat the BPL model of Ref. [59] but with an extra 2 factor in (1) so that  $\Omega_*$  is exactly the peak amplitude at the peak frequency  $f_*$ , while in Ref. [59] the peak amplitude is actually  $\Omega_{\text{BPL}}(f_*) = 2^{(n_2-n_1)/\Delta} \Omega_*$  instead of  $\Omega_*$ . For  $n_2 < 0 < n_1$  and  $\Delta > 0$ , the upper bound  $\Omega_* = 5.6 \times 10^{-7}$  obtained in Ref. [59] with fixed  $n_1 = 3$  and  $\Delta = 2$  actually overestimates the true peak amplitude with a larger overestimation for steeper slopes (larger  $|n_1|$  and/or  $|n_2|$ ) or a wider transition width (a smaller  $\Delta$ ) around the peak position.

In fact, with fixed  $n_1 = 3, n_2 = -1$  ( $n_2 = -4$ ), and  $\Delta = 4$  ( $\Delta = 2$ ) for SGWBs from envelope collisions (sound waves), the 95% upper limit we found on the peak amplitude reads  $\Omega_* < 9.7 \times 10^{-8}$  ( $\Omega_* < 8.2 \times 10^{-8}$ ), which, along with posterior sample of  $f_*$  from the Fig. 4, can be combined into a posterior of  $\Omega_{\text{BPL}}$ , leading to a 95% C.L. constraint  $\Omega_{\text{BPL}}(25 \text{ Hz}) < 3.5 \times 10^{-9}$  ( $\Omega_{\text{BPL}}(25 \text{ Hz}) < 6.4 \times 10^{-9}$ ) at the CBC reference frequency  $f_* = 25$  Hz, while the CBC reference amplitude is found to be bounded by  $\Omega_{\text{ref}} < 5.9 \times 10^{-9}$  ( $\Omega_{\text{ref}} < 5.9 \times 10^{-9}$ ). The Bayes ratios  $\log \mathcal{B}_{\text{Noise}}^{\text{BPL+CBC}} = -1.72$  ( $\log \mathcal{B}_{\text{Noise}}^{\text{BPL+CBC}} = -1.86$ ) and  $\log \mathcal{B}_{\text{CBC}}^{\text{BPL+CBC}} = -1.19$  ( $\log \mathcal{B}_{\text{CBC}}^{\text{BPL+CBC}} = -1.33$ ) even more disfavor for a BPL GW spectrum from envelope collisions (sound waves) over SGWBs from either pure Gaussian noises or CBCs than Ref. [59], slightly improving the previous result.

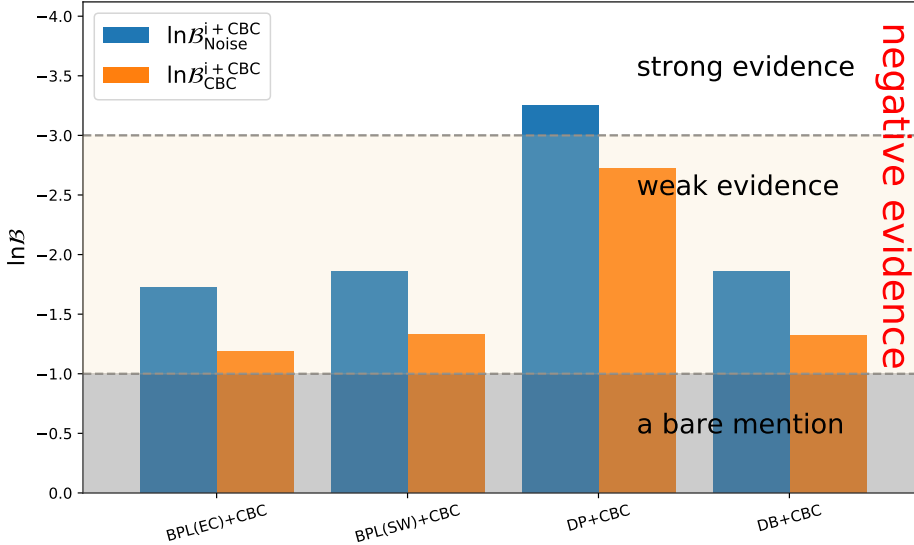


FIG. 2. The Bayes ratios for model comparisons among BPL+CBC models with priors fixed by envelope collisions (EC) and sound waves (SW), DP+CBC model (envelope collisions + sound waves), and DB+CBC model (wall collisions beyond envelope approximation).

### B. The DP+CBC model

For the SGWBs from FOPTs, the present peak frequency of envelope collisions [74, 92–98],

$$\begin{aligned} f_{\text{env}} &= 16.5 \left( \frac{f_{\text{bc}}}{\beta} \right) \left( \frac{\beta}{H_{\text{pt}}} \right) \left( \frac{T_{\text{pt}}}{100 \text{ GeV}} \right) \left( \frac{g_*}{100} \right)^{\frac{1}{6}} \mu\text{Hz} \\ &< 5.775 \left( \frac{\beta}{H_{\text{pt}}} \right) \left( \frac{T_{\text{pt}}}{100 \text{ GeV}} \right) \left( \frac{g_*}{100} \right)^{\frac{1}{6}} \mu\text{Hz}, \end{aligned} \quad (6)$$

is always smaller than the present peak frequency of sound waves [75–77, 99],

$$\begin{aligned} f_{\text{sw}} &= \frac{19}{v_w} \left( \frac{\beta}{H_{\text{pt}}} \right) \left( \frac{T_{\text{pt}}}{100 \text{ GeV}} \right) \left( \frac{g_*}{100} \right)^{\frac{1}{6}} \mu\text{Hz} \\ &> 19 \left( \frac{\beta}{H_{\text{pt}}} \right) \left( \frac{T_{\text{pt}}}{100 \text{ GeV}} \right) \left( \frac{g_*}{100} \right)^{\frac{1}{6}} \mu\text{Hz}, \end{aligned} \quad (7)$$

for the bubble-wall velocity  $0 < v_w < 1$ , where  $f_{\text{bc}} = 0.35\beta/(1 + 0.069v_w + 0.69v_w^4) < 0.35\beta$  is the peak frequency of bubble collisions right after the phase transition,  $\beta/H_{\text{pt}}$  is the Hubble time scale  $H_{\text{pt}}^{-1}$  relative to the PT duration  $\beta^{-1}$  at the PT temperature  $T_{\text{pt}}$ , and  $g_*$  is the effective number of relativistic degrees of freedom. Therefore, we can specifically fix the priors  $f_{*,1} < f_{*,2}$  with  $n_{2,1} = -1, \Delta_1 = 4$  (envelope collisions) and  $n_{2,2} = -4, \Delta_2 = 2$  (sound waves) as well as  $n_{1,i} = 3$  (by causality) for both  $i = 1$  (envelope collisions) and  $i = 2$  (sound waves), and then place 95% C.L. upper limits on the low-frequency peak am-

plitude  $\Omega_{*,1} < 5.8 \times 10^{-8}$  and high-frequency peak amplitude  $\Omega_{*,2} < 4.4 \times 10^{-8}$ , while the CBC reference amplitude is bounded by  $\Omega_{\text{ref}} < 5.6 \times 10^{-9}$  as obtained from Fig. 5. The Bayes ratios  $\log \mathcal{B}_{\text{Noise}}^{\text{DP+CBC}} = -3.25$  and  $\log \mathcal{B}_{\text{CBC}}^{\text{DP+CBC}} = -2.72$  strongly disfavor for the DP+CBC over either noises or CBCs than the single BPL+CBC model does.

The above constraints on the low-frequency and high-frequency peak amplitudes can be transformed into constraints on the PT inverse duration  $\beta/H_{\text{pt}}$  and strength factor  $\alpha$  for a given bubble-wall velocity  $v_w$ . The peak amplitude of envelope collisions is known as [74, 92–98]

$$\Omega_{\text{env}} = 1.67 \times 10^{-5} \frac{A}{h^2} \left( \frac{H_{\text{pt}}}{\beta} \right)^2 \left( \frac{\kappa_\phi \alpha}{1 + \alpha} \right)^2 \left( \frac{100}{g_*} \right)^{\frac{1}{3}}, \quad (8)$$

where  $A(v_w) \equiv 0.48v_w^3/(1 + 5.3v_w^2 + 5v_w^4)$  is the amplitude and  $\kappa_\phi$  is the efficiency factor of inserting released vacuum energy into the bubble wall kinetic energy evaluated generally in Ref. [67]. For the most optimistic constraint, we can take a crude estimation  $\kappa_\phi \approx 1 - \kappa_{\text{sw}}$  from the efficiency factor  $\kappa_{\text{sw}}$  of fluid motions given shortly below. The peak amplitude of sound waves is known as [75–77, 99]

$$\Omega_{\text{sw}} = 2.65 \times 10^{-6} \frac{v_w}{h^2} \left( \frac{H_{\text{pt}}}{\beta} \right) \left( \frac{\kappa_{\text{sw}} \alpha}{1 + \alpha} \right)^2 \left( \frac{100}{g_*} \right)^{\frac{1}{3}} \Upsilon, \quad (9)$$

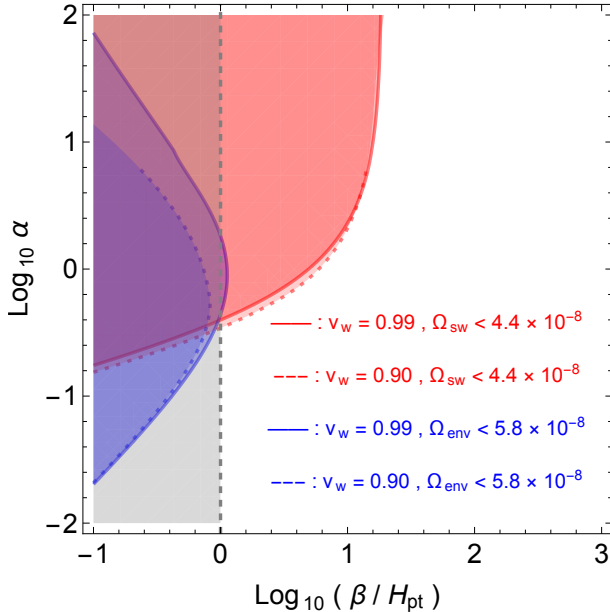


FIG. 3. The implied constraints on the FOPT parameters  $\beta/H_{\text{pt}}$  and  $\alpha$  for the bubble-wall velocities  $v_w = 0.9$  (dashed) and  $v_w = 0.99$  (solid) from the constraints on the DP+CBC model. The blue and red shaded regions are ruled out by the upper bounds on the low-frequency and high-frequency peak amplitudes, respectively. The gray-shaded region is usually not considered for the FOPT to complete successfully.

where the efficiency factor  $\kappa_{\text{sw}}(\alpha, v_w)$  of bulk fluid motions can be fitted as a function of  $\alpha$  and  $v_w$  by hydrodynamics [100] (see also [101] for the varying sound velocity generalization to the constant sound velocity estimations [102–104]). The suppression factor  $\Upsilon \equiv 1 - (1 + 2\tau_{\text{sw}}H_{\text{pt}})^{-1/2}$  [105] accounts for the finite lifetime of sound waves from the onset timescale of turbulence,  $\tau_{\text{sw}}H_{\text{pt}} \approx (8\pi)^{1/3}v_w/(\beta/H_{\text{pt}})\bar{U}_f$ , with the root-mean-squared fluid velocity given by  $\bar{U}_f^2 = 3\kappa_{\text{sw}}\alpha/[4(1+\alpha)]$  [106]. In all cases, we can take the effective number of degrees of freedom  $g_* = 100$  and dimensionless Hubble constant  $h = 0.67$  for illustration. Therefore, both peak amplitudes  $\Omega_{\text{env}}$  and  $\Omega_{\text{sw}}$  can be expressed for a given  $v_w$  as functions of  $\beta/H_{\text{pt}}$  and  $\alpha$ , which can be further constrained in Fig. 3 with the blue and red shaded regions ruled out by  $\Omega_{\text{env}} = \Omega_{*,1} < 5.8 \times 10^{-8}$  and  $\Omega_{\text{sw}} = \Omega_{*,2} < 4.4 \times 10^{-8}$ , respectively. Although the current GW data cannot put strong constraints on the FOPTs, the very strong FOPTs of super-cooling type in the LIGO-Virgo band with  $\alpha \gtrsim \mathcal{O}(1)$  and  $\beta/H_{\text{pt}} \lesssim \mathcal{O}(10)$  can be marginally ruled out from Fig. 3. Note here that there is no precise but conventional definition [107] for the very strong FOPT of super-cooling type. The strength factor  $\alpha$  measures the relative size of released vacuum energy density with respect to the background radiation energy density, and hence  $\alpha \gtrsim \mathcal{O}(1)$  indicates a very strong FOPT. The other parameter  $\beta/H_{\text{pt}}$  measures the relative size of Hubble horizon scale  $H_{\text{pt}}^{-1}$  with respect

to the mean bubble separation  $(8\pi)^{1/3}v_w\beta^{-1} \sim \beta^{-1}$ , and hence  $\beta/H_{\text{pt}} \lesssim \mathcal{O}(10)$  indicates a relatively large radius of bubbles at collisions, which would result in a relatively long PT duration [108, 109] that leads to ultra-low temperature at percolations than the critical/nucleation temperature (hence the name supercooling).

### C. The DB+CBC model

For a physical process associated with two characteristic length scales, the generated SGWBs usually admit a doubly broken (DB) power-law spectrum. One such example is the cosmological FOPT with the vacuum-bubble collisions characterized by the averaged initial bubble separation and bubble-wall thickness, and sound waves characterized by the averaged initial bubble separation and sound shell thickness [71, 78–80]. We consider specifically in this section the GWs from the bubble-wall collisions beyond the envelope approximation with  $n_l = 3$ ,  $n_m = 1$ , and  $n_h = -1$ . The overall amplitude can be constrained as  $\Omega_* < 1.2 \times 10^{-7}$ , which, after combined with the posterior samples of  $f_l$  and  $f_h$  in Fig. 6, renders 95% C.L. upper bound  $\Omega_{\text{DB}}(25 \text{ Hz}) < 2.3 \times 10^{-9}$  at the CBC reference frequency with the corresponding CBC reference amplitude bounded by  $\Omega_{\text{ref}} < 6.0 \times 10^{-9}$ . Similar to the single BPL+CBC model, the Bayes ratios  $\log \mathcal{B}_{\text{Noise}}^{\text{DBBPL+CBC}} = -1.86$  and  $\log \mathcal{B}_{\text{CBC}}^{\text{DB+CBC}} = -1.33$  also slightly disfavor for the DB+CBC over either noises or CBCs.

## V. CONCLUSIONS AND DISCUSSIONS

In this paper, we have implemented the Bayes search for the SGWBs specifically from the cosmological first-order phase transitions with a DP or DB spectrum in the first three observing runs of the Advanced LIGO-Virgo collaborations. No positive evidence has been found for both DP+CBC and DB+CBC models with respective to the backgrounds from either Gaussian noises or CBCs, though the DP+CBC is even more disfavored than the DB+CBC model as well as the usual BPL+CBC model. In particular, our results for the BPL+CBC model slightly improve the previous claim on the null detection for the BPL spectrum, and the DP+CBC results motivated from FOPTs could marginally rule out the very strong FOPT of super-cooling type in the LIGO-Virgo band. All these results could be further improved for the upcoming fourth observing run of the LIGO/Virgo/KAGRA Collaboration, but currently we are still on the way to uncover the SGWBs.

## ACKNOWLEDGMENTS

We thank Huai-Ke Guo, Katarina Martinovic, and Alba Romero for fruitful correspondence on the calibration uncertainties in the LIGO/VIRGO analysis. We thank the helpful discussion on the code with Wen-Hong Ruan, Chang Liu and He Wang. This work is supported by the National Key Research and Development Program of China Grants No. 2021YFC2203004, No.

2021YFA0718304, and No. 2020YFC2201501, the National Natural Science Foundation of China Grants No. 12105344, No.12235019, and No. 12047503, the Key Research Program of the Chinese Academy of Sciences (CAS) Grant No. XDPB15, the Key Research Program of Frontier Sciences of CAS, and the Science Research Grants from the China Manned Space Project No. CMS-CSST-2021-B01. We also acknowledge the use of the HPC Cluster of ITP-CAS.

- 
- [1] B. P. Abbott et al. (LIGO Scientific, Virgo), “GWTC-1: A Gravitational-Wave Transient Catalog of Compact Binary Mergers Observed by LIGO and Virgo during the First and Second Observing Runs,” *Phys. Rev. X* **9**, 031040 (2019), arXiv:1811.12907 [astro-ph.HE].
  - [2] R. Abbott et al. (LIGO Scientific, Virgo), “GWTC-2: Compact Binary Coalescences Observed by LIGO and Virgo During the First Half of the Third Observing Run,” *Phys. Rev. X* **11**, 021053 (2021), arXiv:2010.14527 [gr-qc].
  - [3] R. Abbott et al. (LIGO Scientific, VIRGO, KAGRA), “GWTC-3: Compact Binary Coalescences Observed by LIGO and Virgo During the Second Part of the Third Observing Run,” (2021), arXiv:2111.03606 [gr-qc].
  - [4] J. Aasi et al. (LIGO Scientific), “Advanced LIGO,” *Class. Quant. Grav.* **32**, 074001 (2015), arXiv:1411.4547 [gr-qc].
  - [5] F. Acernese et al. (VIRGO), “Advanced Virgo: a second-generation interferometric gravitational wave detector,” *Class. Quant. Grav.* **32**, 024001 (2015), arXiv:1408.3978 [gr-qc].
  - [6] Nelson Christensen, “Stochastic Gravitational Wave Backgrounds,” *Rept. Prog. Phys.* **82**, 016903 (2019), arXiv:1811.08797 [gr-qc].
  - [7] Arianna I. Renzini, Boris Goncharov, Alexander C. Jenkins, and Pat M. Meyers, “Stochastic Gravitational-Wave Backgrounds: Current Detection Efforts and Future Prospects,” *Galaxies* **10**, 34 (2022), arXiv:2202.00178 [gr-qc].
  - [8] Nick van Remortel, Kamil Janssens, and Kevin Turbang, “Stochastic gravitational wave background: Methods and implications,” *Prog. Part. Nucl. Phys.* **128**, 104003 (2023), arXiv:2210.00761 [gr-qc].
  - [9] Pablo A. Rosado, “Gravitational wave background from binary systems,” *Phys. Rev. D* **84**, 084004 (2011), arXiv:1106.5795 [gr-qc].
  - [10] Xing-Jiang Zhu, E. Howell, T. Regimbau, D. Blair, and Zong-Hong Zhu, “Stochastic Gravitational Wave Background from Coalescing Binary Black Holes,” *Astrophys. J.* **739**, 86 (2011), arXiv:1104.3565 [gr-qc].
  - [11] S. Marassi, R. Schneider, G. Corvino, V. Ferrari, and S. Portegies Zwart, “Imprint of the merger and ringdown on the gravitational wave background from black hole binaries coalescence,” *Phys. Rev. D* **84**, 124037 (2011), arXiv:1111.6125 [astro-ph.CO].
  - [12] C. Wu, V. Mandic, and T. Regimbau, “Accessibility of the Gravitational-Wave Background due to Binary Coalescences to Second and Third Generation Gravitational-Wave Detectors,” *Phys. Rev. D* **85**, 104024 (2012), arXiv:1112.1898 [gr-qc].
  - [13] Xing-Jiang Zhu, Eric J. Howell, David G. Blair, and Zong-Hong Zhu, “On the gravitational wave background from compact binary coalescences in the band of ground-based interferometers,” *Mon. Not. Roy. Astron. Soc.* **431**, 882–899 (2013), arXiv:1209.0595 [gr-qc].
  - [14] Alessandra Buonanno, Gunter Sigl, Georg G. Raffelt, Hans-Thomas Janka, and Ewald Muller, “Stochastic gravitational wave background from cosmological supernovae,” *Phys. Rev. D* **72**, 084001 (2005), arXiv:astro-ph/0412277.
  - [15] Pearl Sandick, Keith A. Olive, Frederic Daigne, and Elisabeth Vangioni, “Gravitational Waves from the First Stars,” *Phys. Rev. D* **73**, 104024 (2006), arXiv:astro-ph/0603544.
  - [16] Stefania Marassi, Raffaella Schneider, and Valeria Ferrari, “Gravitational wave backgrounds and the cosmic transition from Population III to Population II stars,” *Mon. Not. Roy. Astron. Soc.* **398**, 293 (2009), arXiv:0906.0461 [astro-ph.CO].
  - [17] Xing-Jiang Zhu, Eric Howell, and David Blair, “Observational upper limits on the gravitational wave production of core collapse supernovae,” *Mon. Not. Roy. Astron. Soc.* **409**, L132–L136 (2010), arXiv:1008.0472 [gr-qc].
  - [18] Valeria Ferrari, Sabino Matarrese, and Raffaella Schneider, “Stochastic background of gravitational waves generated by a cosmological population of young, rapidly rotating neutron stars,” *Mon. Not. Roy. Astron. Soc.* **303**, 258 (1999), arXiv:astro-ph/9806357.
  - [19] E. Howell, T. Regimbau, A. Corsi, D. Coward, and R. Burman, “Gravitational wave background from sub-luminous GRBs: prospects for second and third generation detectors,” *Mon. Not. Roy. Astron. Soc.* **410**, 2123 (2011), arXiv:1008.3941 [astro-ph.HE].
  - [20] Xing-Jiang Zhu, Xi-Long Fan, and Zong-Hong Zhu, “Stochastic Gravitational Wave Background from Neutron Star r-mode Instability Revisited,” *Astrophys. J.* **729**, 59 (2011), arXiv:1102.2786 [astro-ph.CO].
  - [21] Stefania Marassi, Riccardo Ciolfi, Raffaella Schneider, Luigi Stella, and Valeria Ferrari, “Stochastic background of gravitational waves emitted by magnetars,” *Mon. Not. Roy. Astron. Soc.* **411**, 2549 (2011), arXiv:1009.1240 [astro-ph.CO].
  - [22] Pablo A. Rosado, “Gravitational wave background from rotating neutron stars,” *Phys. Rev. D* **86**, 104007 (2012), arXiv:1206.1330 [gr-qc].
  - [23] Cheng-Jian Wu, Vuk Mandic, and Tania Regimbau, “Accessibility of the stochastic gravitational wave back-

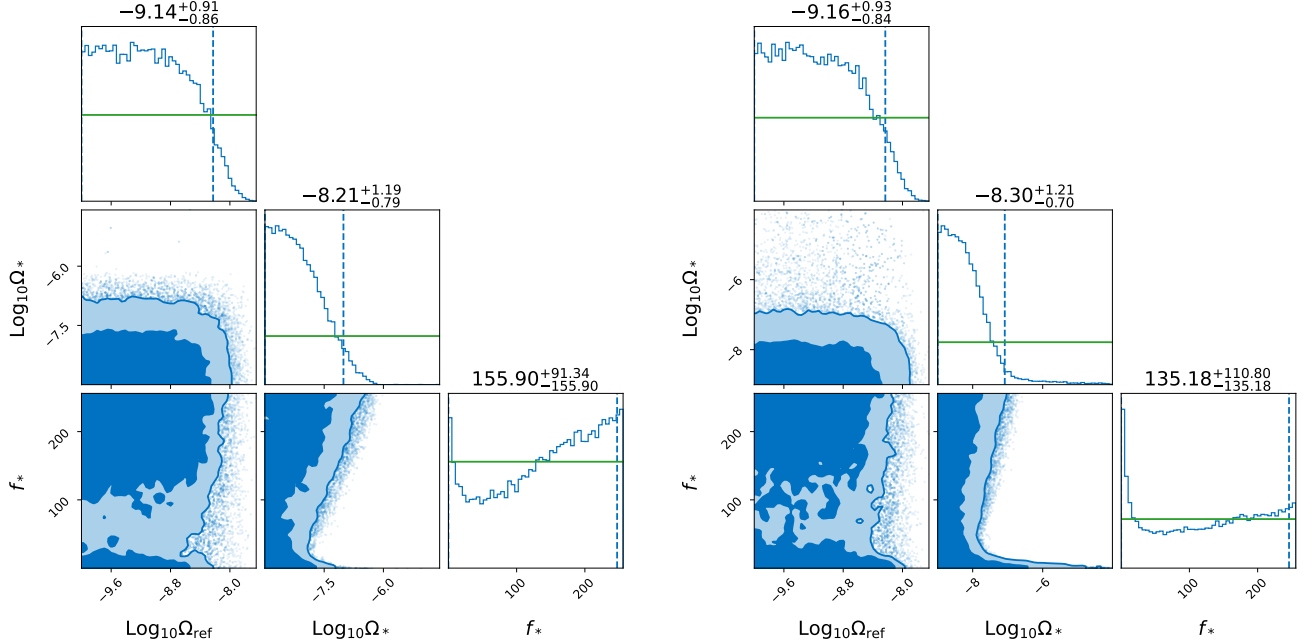


FIG. 4. The parameter posteriors for the BPL+CBC model with BPL priors fixed by envelope collisions (left) and sound waves (right). The 68% and 95% contours are depicted in colors. The vertical dashed lines describe the 95% and the horizon lines are the prior distributions. We also show the (0, 95%) of parameters individually.

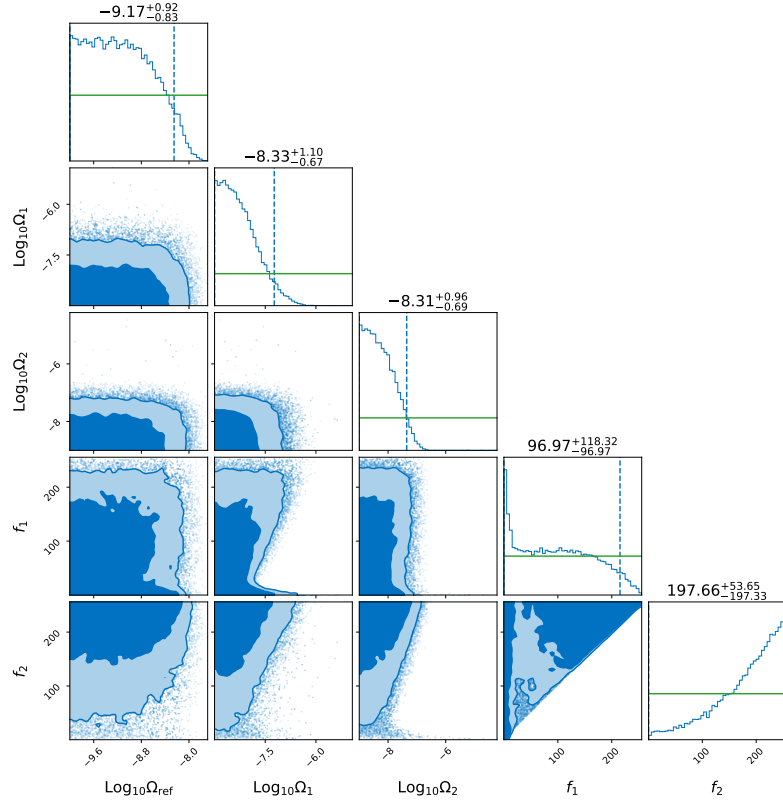


FIG. 5. The parameter posteriors for the BP (envelope collisions + sound waves) + CBC model. The 68% and 95% contours are depicted in colors. The vertical dashed lines describe the 95% and the horizon lines are the prior distributions. We also show the (0, 95%) of parameters individually.

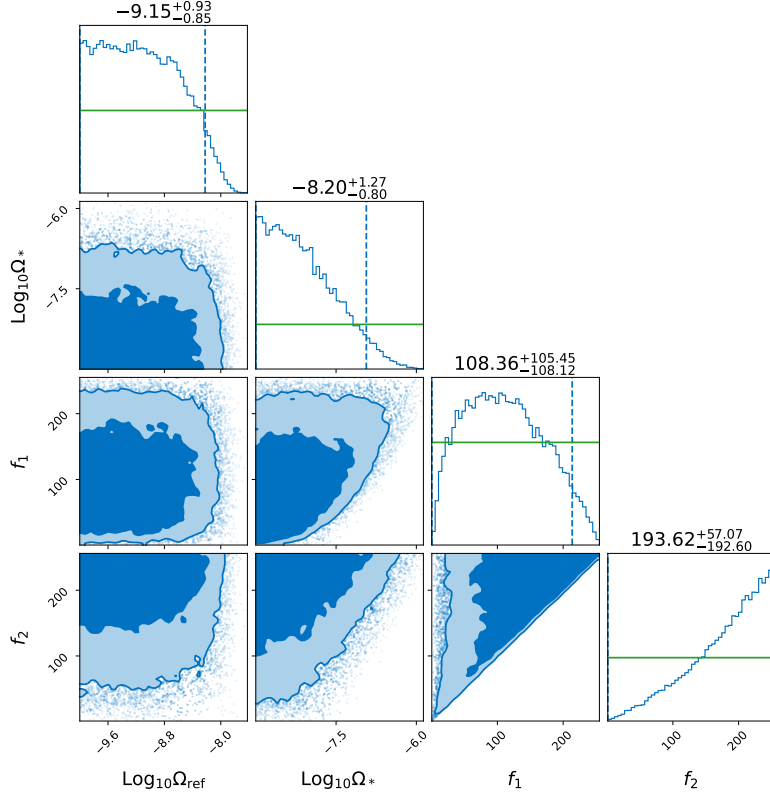


FIG. 6. The parameter posteriors for the DB (beyond envelope)+CBC model. The 68% and 95% contours are depicted in colors. The vertical dashed lines describe the 95% and the horizon lines are the prior distributions. We also show the (0, 95%) of parameters individually.

- ground from magnetars to the interferometric gravitational wave detectors,” Phys. Rev. D **87**, 042002 (2013).
- [24] Paul D. Lasky, Mark F. Bennett, and Andrew Melatos, “Stochastic gravitational wave background from hydrodynamic turbulence in differentially rotating neutron stars,” Phys. Rev. D **87**, 063004 (2013), arXiv:1302.6033 [astro-ph.HE].
  - [25] K. Crocker, V. Mandic, T. Regimbau, K. Belczynski, W. Gladysz, K. Olive, T. Prestegard, and E. Vangioni, “Model of the stochastic gravitational-wave background due to core collapse to black holes,” Phys. Rev. D **92**, 063005 (2015), arXiv:1506.02631 [gr-qc].
  - [26] Kyle Crocker, Tanner Prestegard, Vuk Mandic, Tania Regimbau, Keith Olive, and Elisabeth Vangioni, “Systematic study of the stochastic gravitational-wave background due to stellar core collapse,” Phys. Rev. D **95**, 063015 (2017), arXiv:1701.02638 [astro-ph.CO].
  - [27] Bella Finkel, Haakon Andresen, and Vuk Mandic, “Stochastic gravitational-wave background from stellar core-collapse events,” Phys. Rev. D **105**, 063022 (2022), arXiv:2110.01478 [gr-qc].
  - [28] Richard Brito, Shrobana Ghosh, Enrico Barausse, Emanuele Berti, Vitor Cardoso, Irina Dvorkin, Antoine Klein, and Paolo Pani, “Stochastic and resolvable gravitational waves from ultralight bosons,” Phys. Rev. Lett. **119**, 131101 (2017), arXiv:1706.05097 [gr-qc].
  - [29] Richard Brito, Shrobana Ghosh, Enrico Barausse, Emanuele Berti, Vitor Cardoso, Irina Dvorkin, Antoine Klein, and Paolo Pani, “Gravitational wave searches for ultralight bosons with LIGO and LISA,” Phys. Rev. D **96**, 064050 (2017), arXiv:1706.06311 [gr-qc].
  - [30] Xi-Long Fan and Yan-Bei Chen, “Stochastic gravitational-wave background from spin loss of black holes,” Phys. Rev. D **98**, 044020 (2018), arXiv:1712.00784 [gr-qc].
  - [31] Leo Tsukada, Thomas Callister, Andrew Matas, and Patrick Meyers, “First search for a stochastic gravitational-wave background from ultralight bosons,” Phys. Rev. D **99**, 103015 (2019), arXiv:1812.09622 [astro-ph.HE].
  - [32] Cristiano Palomba et al., “Direct constraints on ultralight boson mass from searches for continuous gravitational waves,” Phys. Rev. Lett. **123**, 171101 (2019), arXiv:1909.08854 [astro-ph.HE].
  - [33] Ling Sun, Richard Brito, and Maximiliano Isi, “Search for ultralight bosons in Cygnus X-1 with Advanced LIGO,” Phys. Rev. D **101**, 063020 (2020), [Erratum: Phys. Rev. D **102**, 089902 (2020)], arXiv:1909.11267 [gr-qc].
  - [34] R. Abbott et al. (KAGRA, VIRGO, LIGO Scientific), “All-sky search for gravitational wave emission from scalar boson clouds around spinning black holes in LIGO O3 data,” Phys. Rev. D **105**, 102001 (2022), arXiv:2111.15507 [astro-ph.HE].
  - [35] Chiara Caprini and Daniel G. Figueroa, “Cosmological Backgrounds of Gravitational Waves,” Class. Quant.

- Grav. **35**, 163001 (2018), arXiv:1801.04268 [astro-ph.CO].
- [36] Rong-Gen Cai, Zhoujian Cao, Zong-Kuan Guo, Shao-Jiang Wang, and Tao Yang, “The Gravitational-Wave Physics,” Natl. Sci. Rev. **4**, 687–706 (2017), arXiv:1703.00187 [gr-qc].
- [37] Ligong Bian et al., “The Gravitational-wave physics II: Progress,” Sci. China Phys. Mech. Astron. **64**, 120401 (2021), arXiv:2106.10235 [gr-qc].
- [38] Michael S. Turner, “Detectability of inflation produced gravitational waves,” Phys. Rev. D **55**, R435–R439 (1997), arXiv:astro-ph/9607066.
- [39] Kouji Nakamura, “Second-order gauge invariant cosmological perturbation theory: Einstein equations in terms of gauge invariant variables,” Prog. Theor. Phys. **117**, 17–74 (2007), arXiv:gr-qc/0605108.
- [40] Kishore N. Ananda, Chris Clarkson, and David Wands, “The Cosmological gravitational wave background from primordial density perturbations,” Phys. Rev. D **75**, 123518 (2007), arXiv:gr-qc/0612013.
- [41] Bob Osano, Cyril Pitrou, Peter Dunsby, Jean-Philippe Uzan, and Chris Clarkson, “Gravitational waves generated by second order effects during inflation,” JCAP **04**, 003 (2007), arXiv:gr-qc/0612108.
- [42] Daniel Baumann, Paul J. Steinhardt, Keitaro Takahashi, and Kiyotomo Ichiki, “Gravitational Wave Spectrum Induced by Primordial Scalar Perturbations,” Phys. Rev. D **76**, 084019 (2007), arXiv:hep-th/0703290.
- [43] Rong-gen Cai, Shi Pi, and Misao Sasaki, “Gravitational Waves Induced by non-Gaussian Scalar Perturbations,” Phys. Rev. Lett. **122**, 201101 (2019), arXiv:1810.11000 [astro-ph.CO].
- [44] Chiara Caprini et al., “Science with the space-based interferometer eLISA. II: Gravitational waves from cosmological phase transitions,” JCAP **04**, 001 (2016), arXiv:1512.06239 [astro-ph.CO].
- [45] Anupam Mazumdar and Graham White, “Review of cosmic phase transitions: their significance and experimental signatures,” Rept. Prog. Phys. **82**, 076901 (2019), arXiv:1811.01948 [hep-ph].
- [46] Chiara Caprini et al., “Detecting gravitational waves from cosmological phase transitions with LISA: an update,” JCAP **03**, 024 (2020), arXiv:1910.13125 [astro-ph.CO].
- [47] Mark B. Hindmarsh, Marvin Lüben, Johannes Lumma, and Martin Pauly, “Phase transitions in the early universe,” SciPost Phys. Lect. Notes **24**, 1 (2021), arXiv:2008.09136 [astro-ph.CO].
- [48] Robert Caldwell et al., “Detection of early-universe gravitational-wave signatures and fundamental physics,” Gen. Rel. Grav. **54**, 156 (2022), arXiv:2203.07972 [gr-qc].
- [49] T. W. B. Kibble, “Topology of Cosmic Domains and Strings,” J. Phys. A **9**, 1387–1398 (1976).
- [50] Saswat Sarangi and S. H. Henry Tye, “Cosmic string production towards the end of brane inflation,” Phys. Lett. B **536**, 185–192 (2002), arXiv:hep-th/0204074.
- [51] Thibault Damour and Alexander Vilenkin, “Gravitational radiation from cosmic (super)strings: Bursts, stochastic background, and observational windows,” Phys. Rev. D **71**, 063510 (2005), arXiv:hep-th/0410222.
- [52] Xavier Siemens, Vuk Mandic, and Jolien Creighton, “Gravitational wave stochastic background from cosmic (super)strings,” Phys. Rev. Lett. **98**, 111101 (2007), arXiv:astro-ph/0610920.
- [53] Sai Wang, Yi-Fan Wang, Qing-Guo Huang, and Tjonne G. F. Li, “Constraints on the Primordial Black Hole Abundance from the First Advanced LIGO Observation Run Using the Stochastic Gravitational-Wave Background,” Phys. Rev. Lett. **120**, 191102 (2018), arXiv:1610.08725 [astro-ph.CO].
- [54] R. Abbott et al. (KAGRA, Virgo, LIGO Scientific), “Upper limits on the isotropic gravitational-wave background from Advanced LIGO and Advanced Virgo’s third observing run,” Phys. Rev. D **104**, 022004 (2021), arXiv:2101.12130 [gr-qc].
- [55] Benjamin P. Abbott et al. (LIGO Scientific, Virgo), “Upper Limits on the Stochastic Gravitational-Wave Background from Advanced LIGO’s First Observing Run,” Phys. Rev. Lett. **118**, 121101 (2017), [Erratum: Phys. Rev. Lett. **119**, 029901 (2017)], arXiv:1612.02029 [gr-qc].
- [56] B. P. Abbott et al. (LIGO Scientific, Virgo), “Search for the isotropic stochastic background using data from Advanced LIGO’s second observing run,” Phys. Rev. D **100**, 061101 (2019), arXiv:1903.02886 [gr-qc].
- [57] B. P. Abbott et al. (LIGO Scientific, Virgo), “Constraints on cosmic strings using data from the first Advanced LIGO observing run,” Phys. Rev. D **97**, 102002 (2018), arXiv:1712.01168 [gr-qc].
- [58] R. Abbott et al. (LIGO Scientific, Virgo, KAGRA), “Constraints on Cosmic Strings Using Data from the Third Advanced LIGO–Virgo Observing Run,” Phys. Rev. Lett. **126**, 241102 (2021), arXiv:2101.12248 [gr-qc].
- [59] Alba Romero, Katarina Martinovic, Thomas A. Calister, Huai-Ke Guo, Mario Martínez, Mairi Sakellariadou, Feng-Wei Yang, and Yue Zhao, “Implications for First-Order Cosmological Phase Transitions from the Third LIGO-Virgo Observing Run,” Phys. Rev. Lett. **126**, 151301 (2021), arXiv:2102.01714 [hep-ph].
- [60] Fei Huang, Veronica Sanz, Jing Shu, and Xiao Xue, “LIGO as a probe of dark sectors,” Phys. Rev. D **104**, 095001 (2021), arXiv:2102.03155 [hep-ph].
- [61] Yang Jiang and Qing-Guo Huang, “Constraining the gravitational-wave spectrum from cosmological first-order phase transitions using data from LIGO-Virgo first three observing runs,” JCAP **06**, 053 (2023), arXiv:2203.11781 [astro-ph.CO].
- [62] Charles Badger et al., “Probing early Universe super-cooled phase transitions with gravitational wave data,” Phys. Rev. D **107**, 023511 (2023), arXiv:2209.14707 [hep-ph].
- [63] Alba Romero-Rodriguez, Mario Martinez, Oriol Pujoles, Mairi Sakellariadou, and Ville Vaskonen, “Search for a Scalar Induced Stochastic Gravitational Wave Background in the Third LIGO-Virgo Observing Run,” Phys. Rev. Lett. **128**, 051301 (2022), arXiv:2107.11660 [gr-qc].
- [64] Bo Mu, Gong Cheng, Jing Liu, and Zong-Kuan Guo, “Constraints on ultraslow-roll inflation from the third LIGO-Virgo observing run,” Phys. Rev. D **107**, 043528 (2023), arXiv:2211.05386 [astro-ph.CO].
- [65] Francesco Bigazzi, Alessio Caddeo, Aldo L. Cotrone, and Angel Paredes, “Dark Holograms and Gravitational Waves,” JHEP **04**, 094 (2021), arXiv:2011.08757 [hep-ph].

- [66] Zizhuo Zhao, Yuefeng Di, Ligong Bian, and Rong-Gen Cai, “Probing the electroweak symmetry breaking history with Gravitational waves,” (2022), arXiv:2204.04427 [hep-ph].
- [67] Rong-Gen Cai and Shao-Jiang Wang, “Effective picture of bubble expansion,” *JCAP* **03**, 096 (2021), arXiv:2011.11451 [astro-ph.CO].
- [68] Rong-Gen Cai, Shi Pi, Shao-Jiang Wang, and Xing-Yu Yang, “Resonant multiple peaks in the induced gravitational waves,” *JCAP* **05**, 013 (2019), arXiv:1901.10152 [astro-ph.CO].
- [69] Jing Liu, Zong-Kuan Guo, Rong-Gen Cai, and Gary Shiu, “Gravitational Waves from Oscillons with Cuspy Potentials,” *Phys. Rev. Lett.* **120**, 031301 (2018), arXiv:1707.09841 [astro-ph.CO].
- [70] Ryusuke Jinno and Masahiro Takimoto, “Gravitational waves from bubble dynamics: Beyond the Envelope,” *JCAP* **01**, 060 (2019), arXiv:1707.03111 [hep-ph].
- [71] Ryusuke Jinno, Thomas Konstandin, and Henrique Rubira, “A hybrid simulation of gravitational wave production in first-order phase transitions,” *JCAP* **04**, 014 (2021), arXiv:2010.00971 [astro-ph.CO].
- [72] Ryusuke Jinno, Thomas Konstandin, Henrique Rubira, and Isak Stomberg, “Higgsless simulations of cosmological phase transitions and gravitational waves,” *JCAP* **02**, 011 (2023), arXiv:2209.04369 [astro-ph.CO].
- [73] Thomas Callister, Letizia Sammut, Shi Qiu, Ilya Mandel, and Eric Thrane, “The limits of astrophysics with gravitational-wave backgrounds,” *Phys. Rev. X* **6**, 031018 (2016), arXiv:1604.02513 [gr-qc].
- [74] Ryusuke Jinno and Masahiro Takimoto, “Gravitational waves from bubble collisions: An analytic derivation,” *Phys. Rev. D* **95**, 024009 (2017), arXiv:1605.01403 [astro-ph.CO].
- [75] Mark Hindmarsh, Stephan J. Huber, Kari Rummukainen, and David J. Weir, “Gravitational waves from the sound of a first order phase transition,” *Phys. Rev. Lett.* **112**, 041301 (2014), arXiv:1304.2433 [hep-ph].
- [76] Mark Hindmarsh, Stephan J. Huber, Kari Rummukainen, and David J. Weir, “Numerical simulations of acoustically generated gravitational waves at a first order phase transition,” *Phys. Rev. D* **92**, 123009 (2015), arXiv:1504.03291 [astro-ph.CO].
- [77] Mark Hindmarsh, Stephan J. Huber, Kari Rummukainen, and David J. Weir, “Shape of the acoustic gravitational wave power spectrum from a first order phase transition,” *Phys. Rev. D* **96**, 103520 (2017), [Erratum: *Phys. Rev. D* 101, 089902 (2020)], arXiv:1704.05871 [astro-ph.CO].
- [78] Mark Hindmarsh, “Sound shell model for acoustic gravitational wave production at a first-order phase transition in the early Universe,” *Phys. Rev. Lett.* **120**, 071301 (2018), arXiv:1608.04735 [astro-ph.CO].
- [79] Mark Hindmarsh and Mulham Hijazi, “Gravitational waves from first order cosmological phase transitions in the Sound Shell Model,” *JCAP* **12**, 062 (2019), arXiv:1909.10040 [astro-ph.CO].
- [80] Rong-Gen Cai, Shao-Jiang Wang, and Zi-Yan Yuwen, “Hydrodynamic sound shell model,” *Phys. Rev. D* **108**, L021502 (2023), arXiv:2305.00074 [gr-qc].
- [81] V. Mandic, E. Thrane, S. Giampaolis, and T. Regimbau, “Parameter Estimation in Searches for the Stochastic Gravitational-Wave Background,” *Phys. Rev. Lett.* **109**, 171102 (2012), arXiv:1209.3847 [astro-ph.CO].
- [82] Thomas Callister, A. Sylvia Biscoveanu, Nelson Christensen, Maximiliano Isi, Andrew Matas, Olivier Minazzoli, Tania Regimbau, Mairi Sakellariadou, Jay Tasson, and Eric Thrane, “Polarization-based Tests of Gravity with the Stochastic Gravitational-Wave Background,” *Phys. Rev. X* **7**, 041058 (2017), arXiv:1704.08373 [gr-qc].
- [83] Patrick M. Meyers, Katarina Martinovic, Nelson Christensen, and Mairi Sakellariadou, “Detecting a stochastic gravitational-wave background in the presence of correlated magnetic noise,” *Phys. Rev. D* **102**, 102005 (2020), arXiv:2008.00789 [gr-qc].
- [84] Andrew Matas and Joseph D. Romano, “Frequentist versus Bayesian analyses: Cross-correlation as an approximate sufficient statistic for LIGO-Virgo stochastic background searches,” *Phys. Rev. D* **103**, 062003 (2021), arXiv:2012.00907 [gr-qc].
- [85] Bruce Allen and Joseph D. Romano, “Detecting a stochastic background of gravitational radiation: Signal processing strategies and sensitivities,” *Phys. Rev. D* **59**, 102001 (1999), arXiv:gr-qc/9710117.
- [86] Ling Sun et al., “Characterization of systematic error in Advanced LIGO calibration,” *Class. Quant. Grav.* **37**, 225008 (2020), arXiv:2005.02531 [astro-ph.IM].
- [87] John T. Whelan, Emma L. Robinson, Joseph D. Romano, and Eric H. Thrane, “Treatment of Calibration Uncertainty in Multi-Baseline Cross-Correlation Searches for Gravitational Waves,” *J. Phys. Conf. Ser.* **484**, 012027 (2014), arXiv:1205.3112 [gr-qc].
- [88] Eric Thrane, Nelson Christensen, and Robert Schofield, “Correlated magnetic noise in global networks of gravitational-wave interferometers: observations and implications,” *Phys. Rev. D* **87**, 123009 (2013), arXiv:1303.2613 [astro-ph.IM].
- [89] Michael W. Coughlin et al., “Measurement and subtraction of Schumann resonances at gravitational-wave interferometers,” *Phys. Rev. D* **97**, 102007 (2018), arXiv:1802.00885 [gr-qc].
- [90] Joshua S. Speagle, “dynesty: a dynamic nested sampling package for estimating Bayesian posteriors and evidences,” *Mon. Not. Roy. Astron. Soc.* **493**, 3132–3158 (2020), arXiv:1904.02180 [astro-ph.IM].
- [91] Gregory Ashton et al., “BILBY: A user-friendly Bayesian inference library for gravitational-wave astronomy,” *Astrophys. J. Suppl.* **241**, 27 (2019), arXiv:1811.02042 [astro-ph.IM].
- [92] Arthur Kosowsky and Michael S. Turner, “Gravitational radiation from colliding vacuum bubbles: envelope approximation to many bubble collisions,” *Phys. Rev. D* **47**, 4372–4391 (1993), arXiv:astro-ph/9211004.
- [93] Arthur Kosowsky, Michael S. Turner, and Richard Watkins, “Gravitational waves from first order cosmological phase transitions,” *Phys. Rev. Lett.* **69**, 2026–2029 (1992).
- [94] Stephan J. Huber and Thomas Konstandin, “Gravitational Wave Production by Collisions: More Bubbles,” *JCAP* **09**, 022 (2008), arXiv:0806.1828 [hep-ph].
- [95] David J. Weir, “Revisiting the envelope approximation: gravitational waves from bubble collisions,” *Phys. Rev. D* **93**, 124037 (2016), arXiv:1604.08429 [astro-ph.CO].
- [96] Daniel Cutting, Mark Hindmarsh, and David J. Weir, “Gravitational waves from vacuum first-order phase transitions: from the envelope to the lattice,” *Phys.*

- Rev. D **97**, 123513 (2018), arXiv:1802.05712 [astro-ph.CO].
- [97] Daniel Cutting, Elba Granados Escartin, Mark Hindmarsh, and David J. Weir, “Gravitational waves from vacuum first order phase transitions II: from thin to thick walls,” Phys. Rev. D **103**, 023531 (2021), arXiv:2005.13537 [astro-ph.CO].
- [98] Oliver Gould, Satumaaria Sukuvaara, and David Weir, “Vacuum bubble collisions: From microphysics to gravitational waves,” Phys. Rev. D **104**, 075039 (2021), arXiv:2107.05657 [astro-ph.CO].
- [99] Daniel Cutting, Mark Hindmarsh, and David J. Weir, “Vorticity, kinetic energy, and suppressed gravitational wave production in strong first order phase transitions,” Phys. Rev. Lett. **125**, 021302 (2020), arXiv:1906.00480 [hep-ph].
- [100] Jose R. Espinosa, Thomas Konstandin, Jose M. No, and Geraldine Servant, “Energy Budget of Cosmological First-order Phase Transitions,” JCAP **06**, 028 (2010), arXiv:1004.4187 [hep-ph].
- [101] Shao-Jiang Wang and Zi-Yan Yuwen, “The energy budget of cosmological first-order phase transitions beyond the bag equation of state,” JCAP **10**, 047 (2022), arXiv:2206.01148 [hep-ph].
- [102] Felix Giese, Thomas Konstandin, and Jorinde van de Vis, “Model-independent energy budget of cosmological first-order phase transitions—A sound argument to go beyond the bag model,” JCAP **07**, 057 (2020), arXiv:2004.06995 [astro-ph.CO].
- [103] Felix Giese, Thomas Konstandin, Kai Schmitz, and Jorinde van de Vis, “Model-independent energy budget for LISA,” JCAP **01**, 072 (2021), arXiv:2010.09744 [astro-ph.CO].
- [104] Xiao Wang, Fa Peng Huang, and Xinmin Zhang, “Energy budget and the gravitational wave spectra beyond the bag model,” Phys. Rev. D **103**, 103520 (2021), arXiv:2010.13770 [astro-ph.CO].
- [105] Huai-Ke Guo, Kuver Sinha, Daniel Vagie, and Graham White, “Phase Transitions in an Expanding Universe: Stochastic Gravitational Waves in Standard and Non-Standard Histories,” JCAP **01**, 001 (2021), arXiv:2007.08537 [hep-ph].
- [106] David J. Weir, “Gravitational waves from a first order electroweak phase transition: a brief review,” Phil. Trans. Roy. Soc. Lond. A **376**, 20170126 (2018), arXiv:1705.01783 [hep-ph].
- [107] Xiao Wang, Fa Peng Huang, and Xinmin Zhang, “Phase transition dynamics and gravitational wave spectra of strong first-order phase transition in supercooled universe,” JCAP **05**, 045 (2020), arXiv:2003.08892 [hep-ph].
- [108] Rong-Gen Cai, Misao Sasaki, and Shao-Jiang Wang, “The gravitational waves from the first-order phase transition with a dimension-six operator,” JCAP **08**, 004 (2017), arXiv:1707.03001 [astro-ph.CO].
- [109] John Ellis, Marek Lewicki, and José Miguel No, “On the Maximal Strength of a First-Order Electroweak Phase Transition and its Gravitational Wave Signal,” JCAP **04**, 003 (2019), arXiv:1809.08242 [hep-ph].